Iraqi National Journal of Earth Science

www.earth.mosuljournals.com

Geotechnical Investigation on the Right Side of Mosul City by ArcGIS

Eman K. Al-Ojar [1*], Azealdeen S. Al-Jawadi [2], Abdulsalam M. Altarif [3]

[1,2] Department of Mining, College of Petroleum and Mining Engineering, University of Mosul, Mosul, Iraq.
[3] Department of Applied Geology, College of Science, University of Tikrit, Tikrit, Iraq.

Article information

Received: 29- June -2024

Revised: 30- Jul -2024

Accepted: 06- Sep -2024

Available online: 01- Jul – 2025

Keywords:
Mosul
Right side
Geotechnique
GIS
Investigation

Correspondence:
Name: Eman K. Al-Ojar
Email: eman.q@uomosul.edu.iq

ABSTRACT

Military efforts to evict terrorist organizations from the governorate caused widespread destruction in Mosul, particularly on the right side of the Tigris River. The city required a complete reconstruction of its buildings and infrastructure. Geotechnical investigations were carried out in the majority of the right-side areas in preparation for the sewerage projects. 64 boreholes were drilled to a depth of 5 m. During the drilling, the physical and engineering properties investigations of the soil have been studied, and the vertical soil depths are divided into three beds (1.5, 3, and 5 m). The investigation was done by the Al-Mawarid Bureau for geological and engineering geology investigations. The data are interpolated by spatial analysis tools in the ArcGIS application using the Ordinary Kriging Method (OK), which is a better method to represent distribution values nearest to the actual values compared with other methods of interpolation. The results indicate that the soil was distributed into three groups: high plasticity clay, low plasticity clay, and low plasticity silt. Most areas have a liquid limit between 30-50%, a decreased plasticity index toward deeper layers, and low clay activity, while the swelling potential is high except in the southeastern part of the study area, where the bearing capacity increases with depth. In the northeast, the foundation type is compact footing with 1.8 m depth, and in the southwest, it needs a deep pile with 5 m depth. While the chemical test of the soil in the study area has an intensive sulfate environment and the chloride content is between (0.03-0.04) %.

DOI: 10.33899/earth.2025.152379.1326,

التحريات الجيوتكنيكية في الجانب الأيمن لمدينة الموصل باستخدام برنامج ArcGIS

ايمان قاسم الاوجار [1*]، عزالدين صالح الجوادي [2]، عبدالسلام مهدي الترف [3]

[2,1]قسم التعدين، كلية هندسة النفط والتعدين، جامعة الموصل، الموصل، العراق.

[3]قسم علوم الأرض التطبيقية، كلية العلوم، جامعة تكريت، تكريت، العراق.

معلومات الارشفة

تاريخ الاستلام: 29- يونيو -2024

تاريخ المراجعة: 30- يوليو -2024

تاريخ القبول: 06- سبتمبر -2024

تاريخ النشر الالكتروني: 01- يوليو -2025

الكلمات المفتاحية:

الموصل

الجانب الأيمن

الجيوتكنيك

نظم المعلومات الجغرافية

التحريات

المراسلة:

الاسم: ايمان قاسم الاوجار

Email: eman.q@uomosul.edu.iq

الملخص

تسببت العمليات العسكرية لطرد التنظيمات الإرهابية من المحافظة في إحداث دمار واسع النطاق في الموصل، وخاصة في الجانب الأيمن من نهر دجلة. وتطلبت المدينة إعادة بناء كامل لمبانيها وبناها التحتية. وقد أجريت تحقيقات جيوتقنية في غالبية مناطق الجانب الأيمن استعداداً لمشاريع الصرف الصحي. وتم حفر 64 بئراً بعمق 5 أمتار. وخلال الحفر، تمت دراسة خواص التربة الفيزيائية والهندسية، وتم تقسيم أعماق التربة افقيا إلى ثلاث طبقات (1.5 و3 و5) أمتار. وقد تم إجراء التحريات من قبل مكتب الموارد للتحقيقات الجيولوجية والهندسية. وتم استكمال البيانات بواسطة أدوات التحليل المكاني في تطبيق ArcGIS، باستخدام طريقة كريجنج الاعتيادية، والتي كانت الطريقة الأفضل لتمثيل توزيع القيم الأقرب إلى القيم الفعلية مقارنة بطرق الاستيفاء الأخرى. وظهرت النتيجة أن التربة توزعت إلى ثلاث مجموعات: طين عالي اللدونة، وطين منخفض اللدونة، وطمي منخفض اللدونة. ومعظم المناطق لها حد سيولة يتراوح ما بين (30-50%) ومعامل لدونة منخفض نحو الطبقات الاعمق، وان فعالية الاطيان منخفضة بينما لها جهد انتفاخ عالٍ ما عدا الجزء الجنوبي الشرقي حيث تزداد قدرة التحمل مع العمق. ففي الجزء الشمالي الشرقي يتطلب نوع الأساس أساساً مضغوطاً بعمق 1.8 م، وفي الجنوب الغربي يحتاج إلى ركيزة عميقة بعمق 5 م، بينما اظهرت التحليل الكيميائية للتربة في منطقة الدراسة ان البيئة عالية الكبريتات ومحتوى الكلوريد فيها يتراوح ما بين (0.03-0.04)%.

DOI: 10.33899/earth.2025.152379.1326,

Introduction

Geotechnical investigation is an essential component of civil engineering projects, although it is frequently disregarded for a variety of reasons, including ignorance, carelessness, or a lack of funding (Ikara et al., 2019). A new technique for data collecting, archiving, organizing, retrieving, visualizing, and analyzing various kinds of site investigations was developed by geological and geographical engineers. The GIS can be used to display digital maps and other graphic data to analyze, present, and create the ideal vision for the designer (Aldefae et al., 2020).

Mosul City is the center of Nineveh Governorate in Iraq (Fig. 1). It has cultural and historical significance as many historical eras have passed through it for thousands of years. It was exposed to many instances of demolition and reconstruction over that time due to warfare and natural disasters; the most recent was the war in 2017, which was caused by the terrible devastation and left the majority of the right side in ruins. So, the local government of Nineveh is giving great attention to reconstructing the right side of Mosul City and creating compounds and districts. As a result, it has become necessary to carry out underground geotechnical studies. The map generated by the United Nations Institute for Training and Research (UNITAR) shows that the old Mosul City sustained the greatest damage. The western parts of Mosul suffered the most damage, as shown in Figure 2, which displays a map of Mosul with estimated building damage (UN-Habitat, 2019; Boloorani et al., 2021). Over 1.5 million tons of construction debris from the military strikes are located in the old city, as shown in the damaged areas. It is found through field surveys that every five square meters contains a ton of building bonding material and pieces of gypsum, while every four square meters contains a ton

of building stones, and every forty square meters contains a volume of one cubic meter of gypsum stones (Al-Jawadi *et al.*, 2022).

Specifying recycling and disposal facilities along with instructions for clearing debris will help the continuous self-rebuilding process. The municipal authorities must impose official consent and guidelines on the property owners before demolishing the remains (Abdulrazaq and Guedes, 2021). It is essential to study and use previous experiences acquired in reconstructing cities devastated by natural disasters and wars for the reconstruction of Mosul. One of these cities is Warsaw in Poland that exposed to destruction in the Second World War, as well as the systematic eradication of identity and legacy by Nazi Germans who attempted to destroy Warsaw's cultural and civilizational landmarks to obliterate the city's identity (Alrobaee and Al Yousif, 2018). However, the citizens of the city insisted on preserving its history and reconstructing it inside the urban framework (Kobylarczyk et al, 2020). Another case is in the Ahr Valley, while more than 220 people lost their lives in July 2021 flood disaster in Western and Central Europe; the Ahr Valley in Germany was particularly severely affected, with at least 135 people losing their lives, over 9,000 buildings damaged or destroyed, and billions of euros in damages. Authors recommend that when considering exposure and relocation, not to use events with a statistical return period of one hundred years as the design events, but rather extreme events. To avoid destruction and suggest that the needs of particularly vulnerable population groups can be taken into account more strongly and systematically in reconstruction and new construction (Truedinger et al., 2024).

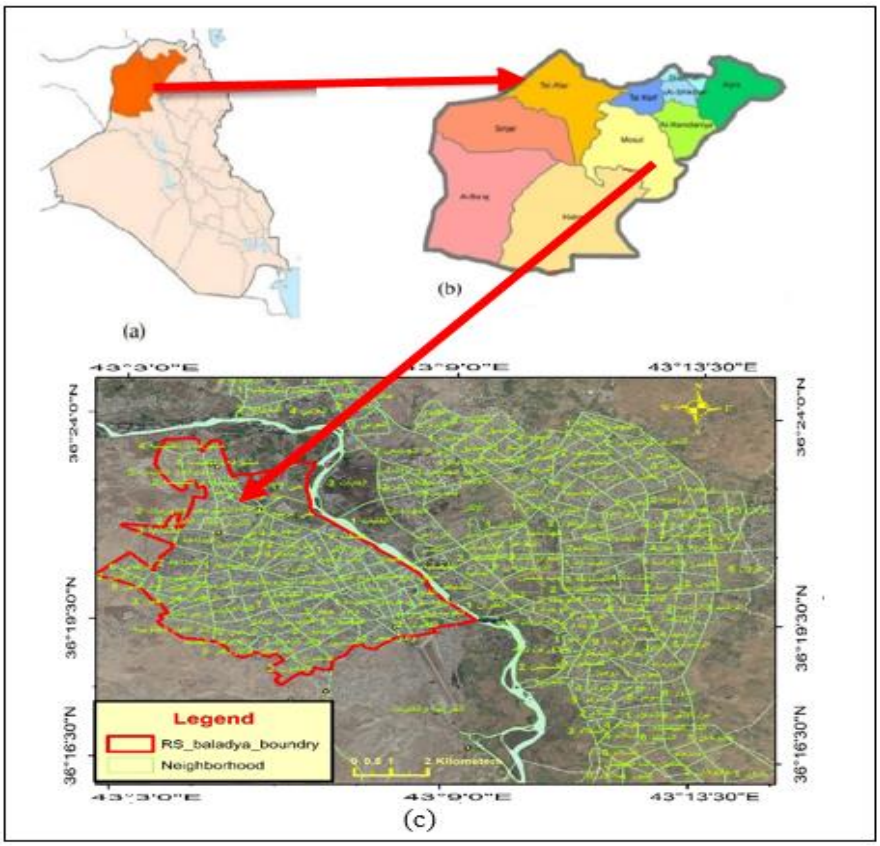

Fig. 1. a) Location of Nineveh Governorate in Iraq; b) Location of Mosul City from the administrative units for the Nineveh Governorate; c) the right-side districts of Mosul City.

The sustainable integration of city reconstruction plans is ordering the reconstruction process and placing solutions according to their significance, establishing the reconstruction project's tactics to be a sustainable, balanced process, and assessing it in light of the reconstruction theory's theoretical foundation and prior global experiences (Kawther and Hassan, 2022).

The level of destruction caused by human strife in cities is at its highest point since World War II. Cities have evolved into the main theaters of conflict, with extensive destruction seen in a variety of locations, including Timbuktu, Sarajevo, Beirut, Aleppo, Raqqa, Misurata, Gaza, Mosul, Donetsk, and Marawi. Key variables that either facilitate or obstruct responsible reconstruction in cities

experiencing intense or protracted war have been identified by War in Cities and the Centre for Urban Conflicts Research (UCR) (Pullan and Azzouz, 2019).

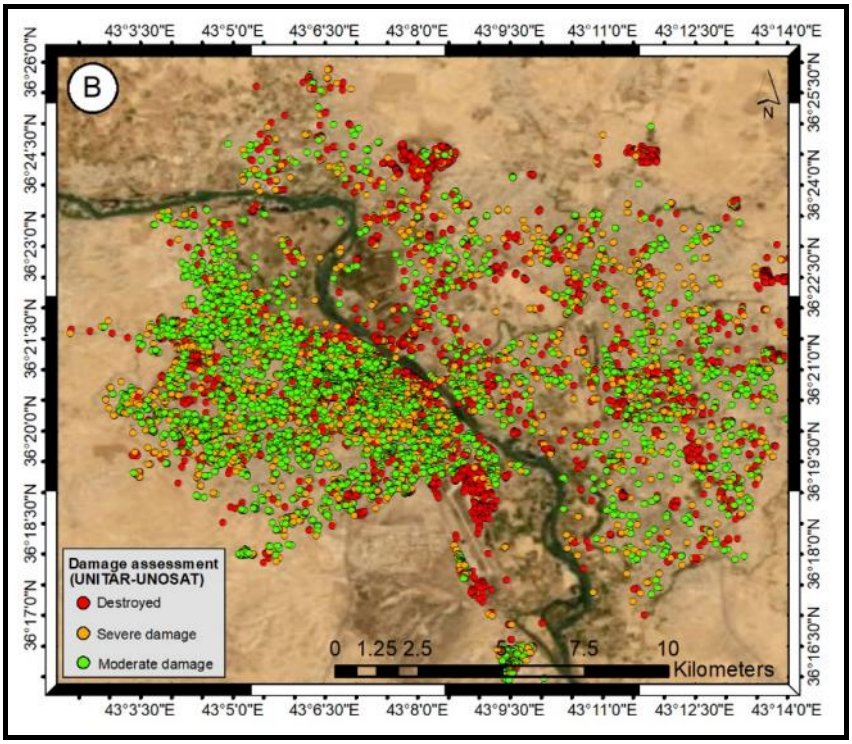

Fig. 2. Map of Mosul City showing the estimated building damage (Boloorani et al., 2021) according to UN Habitat (2019).

Fig. 3. Old Mosul City before and after the destruction and targeting operation by war (Al-Mosawy et al., 2021).

The geostatistical analyzer extension in ArcMap is used to interpolate geotechnical data and forecast data at unknown locations. Kriging is a type of spatial interpolation method that makes predictions at unsampled locations using a linear combination of observations at nearby sampled locations (Ikara et al., 2022). Kriging is regarded as the best geostatistical interpolator since the predicted squared difference between the estimated and known value is minimal for all linear estimators. Since it specifies that the expected error is equal to zero, it is an unbiased estimator (Boumpoulis et al., 2023). The Ordinary Kriging (OK) is employed in this investigation, and it is found that OK gives better results for the spatial interpolation distribution. The study aims to make geotechnical maps based on physical and engineering properties of the soil using the spatial interpolation method in the ArcGIS program. This is due to the covered areas that have not been tested, and gives them estimated statistical values to save effort and money, and to give a preliminary idea about the geotechnical properties of the soil for planning the area before starting reconstruction.

Geological setting

The Fatha Formation (Middle Miocene) and Quaternary sediments cover the study area, where the Fatha Formation consists of alternating cycles of limestone, silt, green marl or marly clay, gypsum or anhydrite, and limestone. This formation is 190–170 meters thick in the Mosul region, and it gets thinner towards the northeast (Source). The existence of the Fatha Formation affects on geological characteristics of the right side. It is composed of successions of limestone, swellable marl, and dissolvable gypsum. The floodplain of most of the region on the right side close to the river is made up of the Quaternary deposits, also known as the floodplain and river terraces (AL-Jaber, 1997). From a tectonic standpoint, several faults damaged Mosul City, affecting both the urban distribution and the geotechnical characteristics of the rocks (Al-Jawadi et al., 2022). Figure 4 shows a structural map modified from Adeeb (1988).

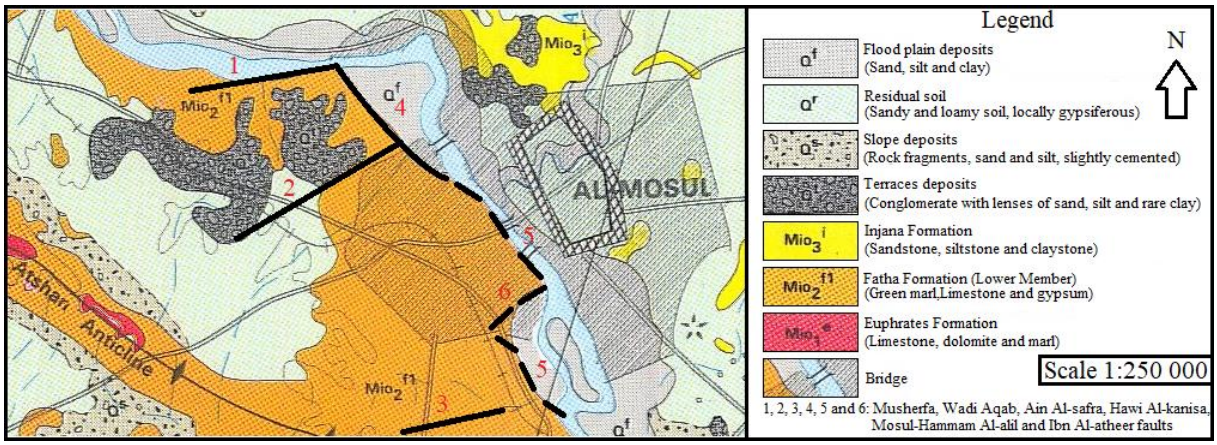

Fig. 4. Mosul geological and structural map (modified from Adeeb, 1988, and Sissakian et al., 1995).

Methodology

Borehole Location:

The boreholes were located in the field by a GPS handheld based on the coordinates obtained from the proposed project provided by the design for 64 boreholes (Fig. 5).

Laboratory tests:

A geotechnical laboratory test for determining physical, mechanical, and chemical properties was carried out on the soil samples obtained from 64 boreholes drilled during the work on soil investigation of the site for the right-side sewage project in Mosul district, Nineveh Governorate. Al-Mawarid Company, Geological and Engineering Consultation Bureau, implemented the project at the request of Shams Construction Company. The actual test proposed for a particular sample depends on the type of sample, Undisturbed Samples (US), Disturbed Samples (DS), and Split Spoon Samples (SS), and the nature of their materials. The procedures of all tests are shown in Table 1.

The current study was based on the Unified Soil Classification System (USCS) and through volumetric analysis based on the specifications that were conducted. Grain size distribution curves for soil samples taken from in situ boreholes were determined using sieve analysis to find the percentage fraction by weight according to ASTM D-2488 and ASTM D-2487.

Laboratory physical tests consist of Atterberg Limits to determine Liquid Limit (LL), Plastic Limit (PL), Plasticity Index (PI), as well as Water Content (w), and Specific Gravity (G).

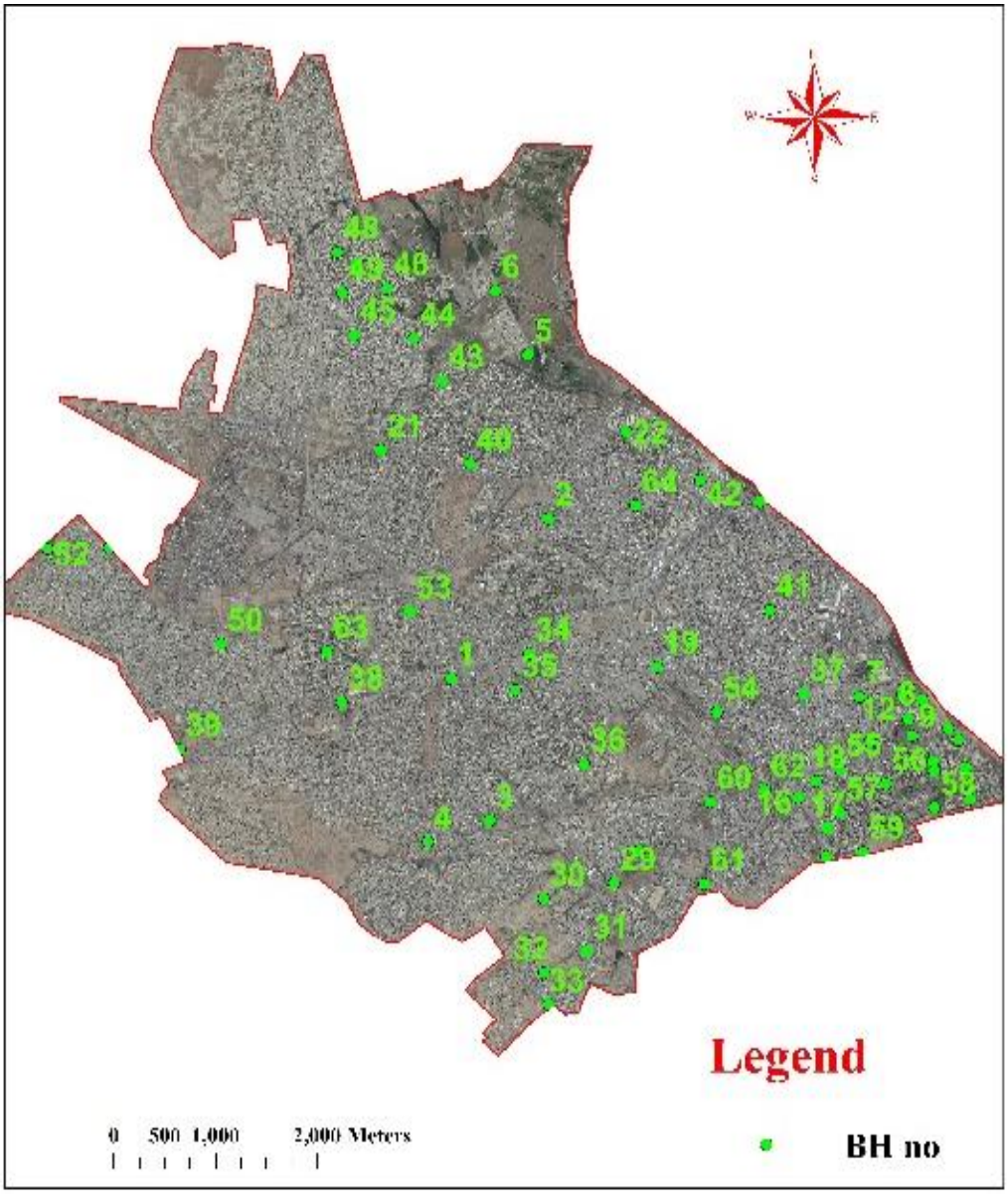

Fig. 5. Location of boreholes in the study area on the right side of Mosul City.

Table 1. Summary of Laboratory Testing.

Type	Test		Testing Standard
Classification Tests	Atterberg Limits (LL and PI)		ASTM D 4318
	Grain Size Analysis	Sieve	ASTM D 422
		Hydrometer	
Type of samples	Disturbed samples (DS)		ASTM D -1586
	Undisturbed Samples (US)		ASTM D-1587
	Split Spoon Samples (S.S)		ASTM D 1586-99
Physical Properties	Specific Gravity		ASTM D 854
	Natural Water Content		ASTM D 2216
	Unit Weight		BS1377:1990
SPT	Standard penetration test		ASTM D 1586-99
Chemical Test	Gypsum		. BS 1377: 1990 Part 3 • ASTM • Earth Manual
	Sulphate Content		
	Organic Matter Content		
	Total Soluble Salts (TSS)		
	Chloride Content		
	pH, Cl, SO_4, and TDS for Water		

LL is the liquid limit; PI is the plasticity index

Results and Discussion

Physical properties:

Grain size

The results are shown by drawing a map of the granular size distribution based on spatial interpolation using the OK method in the program according to ArcGIS.

In the first bed B1 (1-1.5 m), the size of the gravel and sand is higher in the valley areas between (5-14%) and (32-62%) respectively (Fig. 6 a,b) resulting from the faults of Wadi Akkab, Wadi Hajar and Wadi Al-Ain (Fig. 5). While the percentage of finer materials in this bed decreases in the valleys areas, the percentage of clays and silt is between (19 - 33.5%) and (3-25%) respectively (Fig. 6 c,d).

In the second bed B2 (to 3m), the percentage of gravel and sand grain sizes in the valley areas decreases, ranging between 0-4% and 10-20% (Fig. 7a, b). The percentage of silt and clay increases to (20-30%) and (32-62%) (Fig. 7c,d); further, the increase is greater in the floodplain areas for the gravel sizes reaching (21%). The sand percentage increases to (20-40%), and a slight decrease appears for clay and silt size, as its percentage is between (10-40%) and (10-30%) (Fig. 7a,b).

In the third bed B3 (to 5m), a significant decrease is noticed in the gravel sizes in the valley areas also in the floodplain areas approaching (0-3%) as shown in figure (8a), and the size percentage increased in the center part of the study between (3-5%) and a slight increase is observed in the southeastern part. This increase is caused by allowing heavy load deposition from the river meander and narrows in this area, as an increase in gravel and sand size percentage in the north-west of the study area. Moreover, a gradient decrease in the distribution of sand and gravel is recognized towards the west of the study area (Fig. 8a, b). A decrease in the percentages of silt particle size appeared in almost all areas except the southeastern part (Fig. 8c), while the clay percentage increases in the valley areas and decreases in the other parts (Fig. 8d). The increase and decrease at the vertical level of all depth layers in the region of the fault are attributed to the increasing grain size gradient towards up.

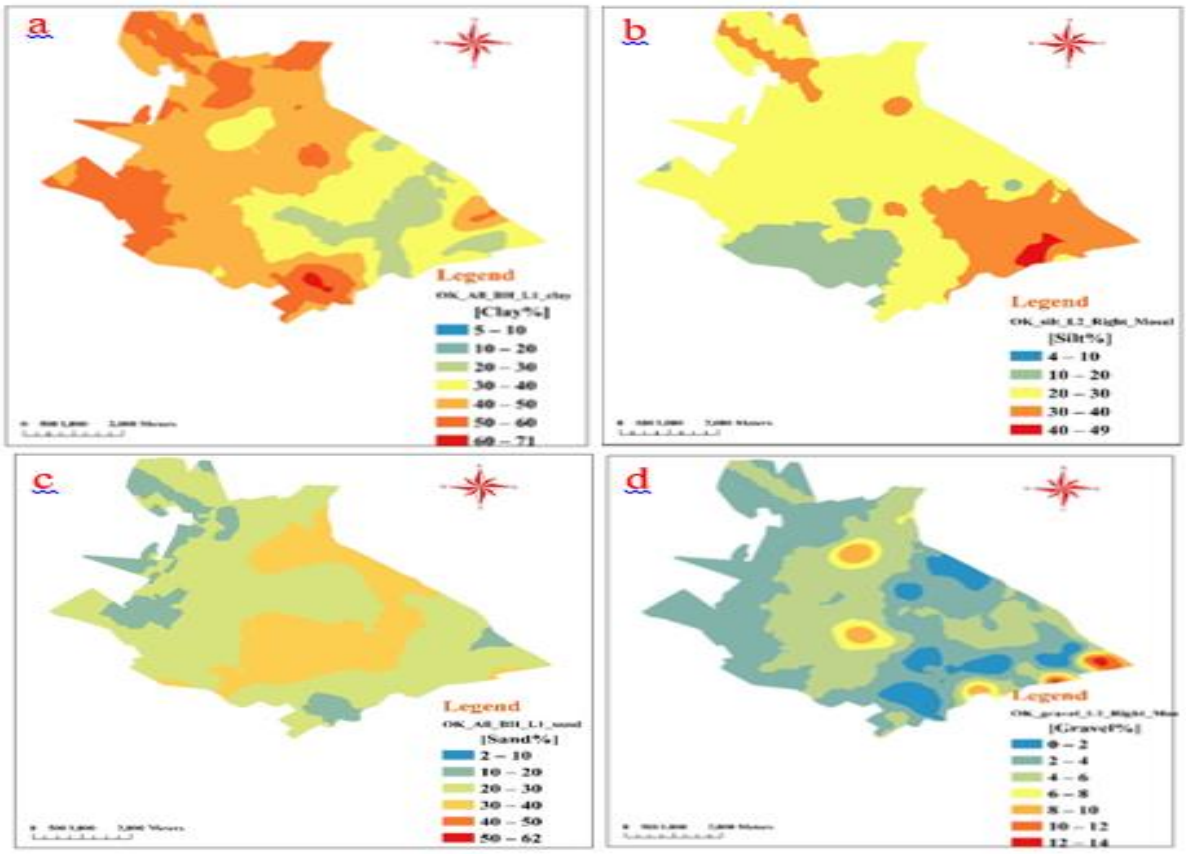

Fig. 6. Grain size distribution at layer one (1-1.5m) by interpolation in the ArcGIS program; a- clay, b- silt, c- sand, d- gravel.

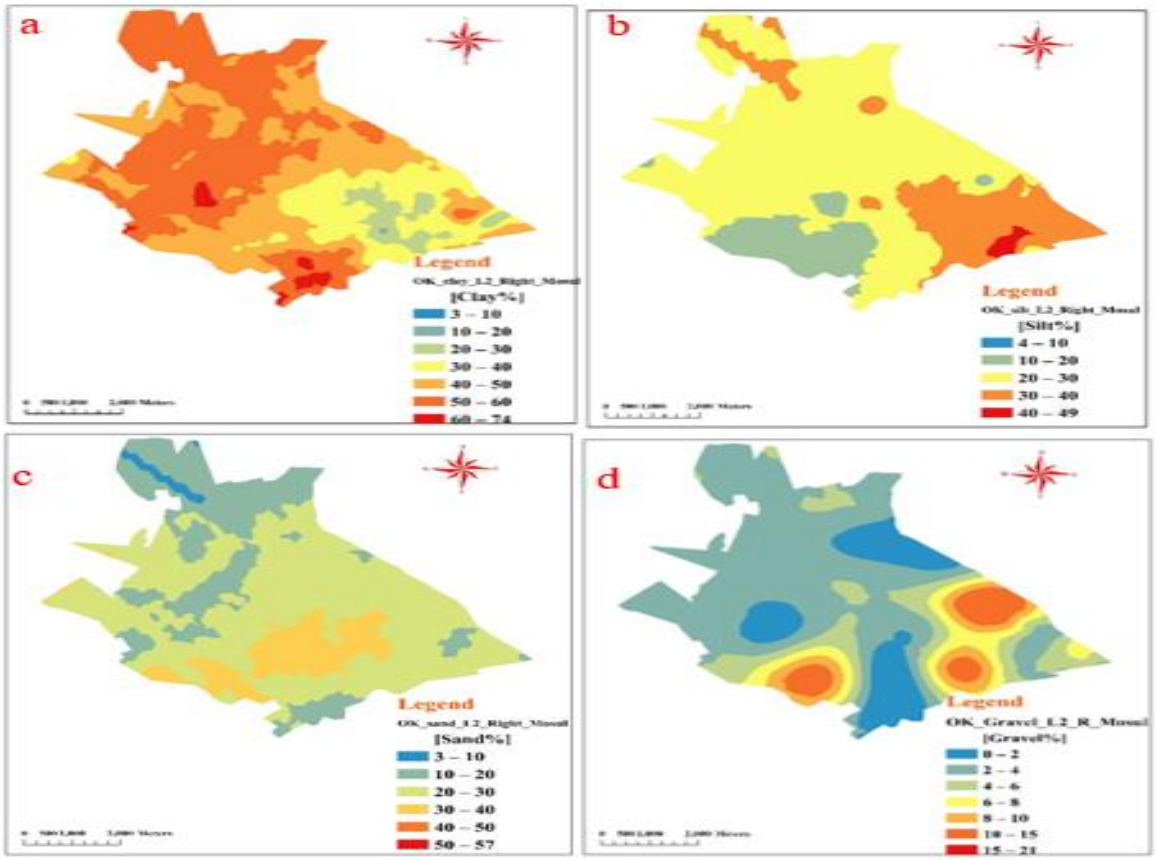

Fig. 7. Grain size distribution at layer two (to 3m) by interpolation in the ArcGIS program; a- clay, b- silt, c- sand, d- gravel.

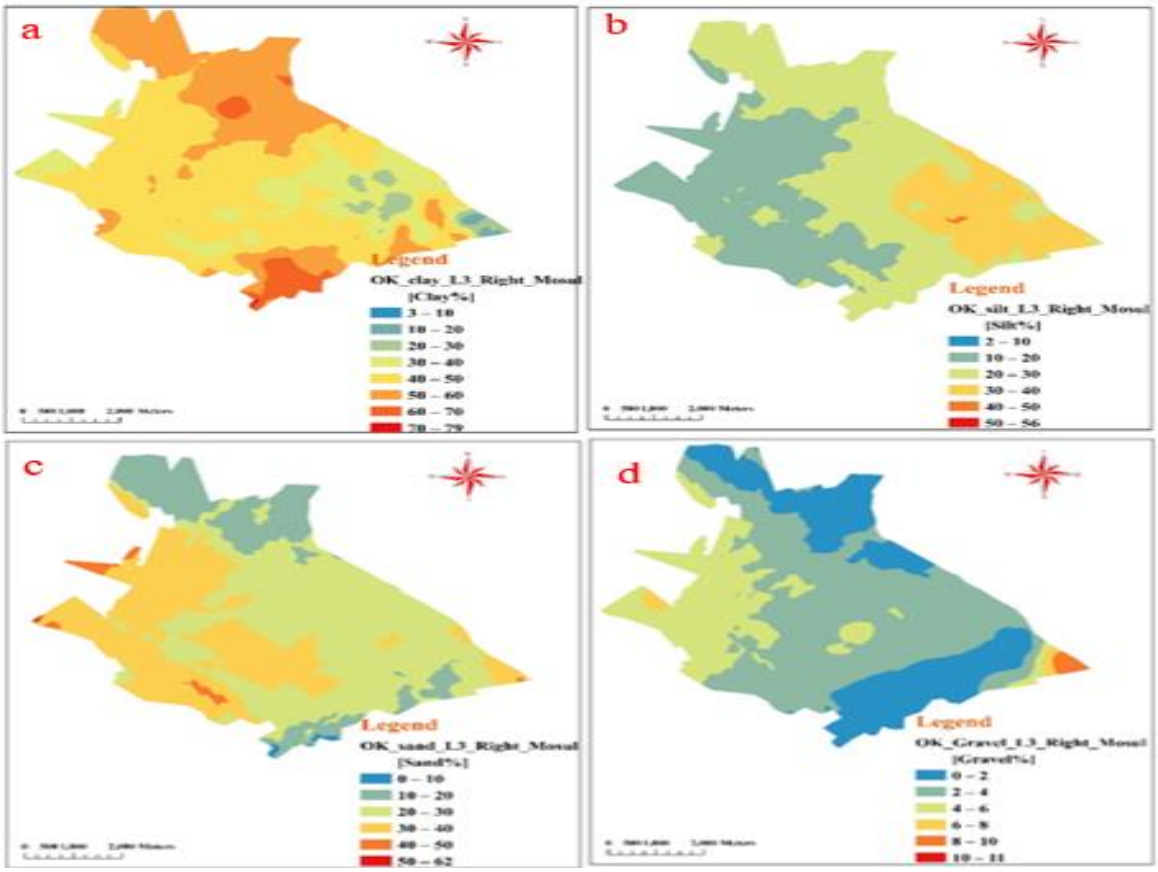

Fig. 8. Grain size distribution at layer three (to 5m) by interpolation in the ArcGIS program; a- clay, b- silt, c- sand, d- gravel.

Atterberg Limits

The results for the three layers on the plasticity chart show that the data are distributed over three groups: (CH- high plasticity clay), (CL- Low plasticity clay), and (ML- low plasticity silt) (Figs. 9, 10, 11).

Using the interpolation OK method in the ArcGIS program, bed one shows the liquid limit percentage between (30–50%) distributed at most study areas, and decreased in the area near the river, as in Figure 12a. Moreover, a liquidity limit of between (30-50%) covered a great part of the study area for bed two, except a few parts have a plasticity limit over (50%), and very few parts of the study areas have a liquid limit of less than (30%) (Fig. 9 b); however, liquidity limit ratio between (30-50%) dominated at bed three (Fig. 12 c).

The plasticity index can be expressed practically as the difference between the fluidity and plasticity limits, since the plasticity index shows the moisture content at which the soil starts to plasticize. Applying spatial interpolation by OK, most of the area has a plasticity limit between (20–30%) and an increased percentage of more than (30%) at the eastern part of the study area's center and a higher decreasing in the southern part of the study area between (10–20%) (Fig. 13).

At the second bed, the PI values are variable; the values less than 20% are dominant in most of the southern areas, where PI values increased between 20-30% towards the northern part of the study area. The appearance values of more than 30% along the middle areas and stretch at the west with the presence in the southwestern areas, also a small part of the southeast of the study area (Fig. 13 b).

PI values typically range from (20–30%) for most areas of the third bed, except a very small part of the southern east while the PI values are between (10-20%) and some scattered parts in the eastern north and western south have PI values more than (30%) (Fig. 13 c).

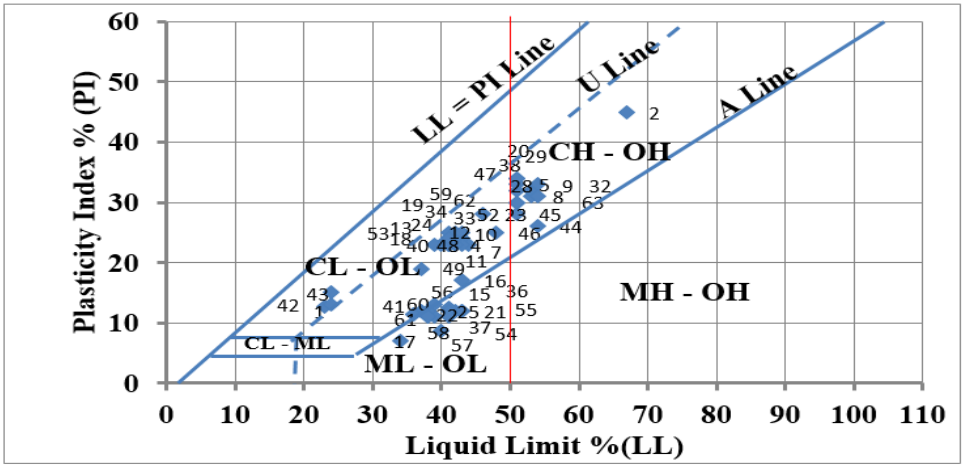

Fig. 9. Plasticity chart of soil in the study area of layer one B1 depth (1-1.5 m).

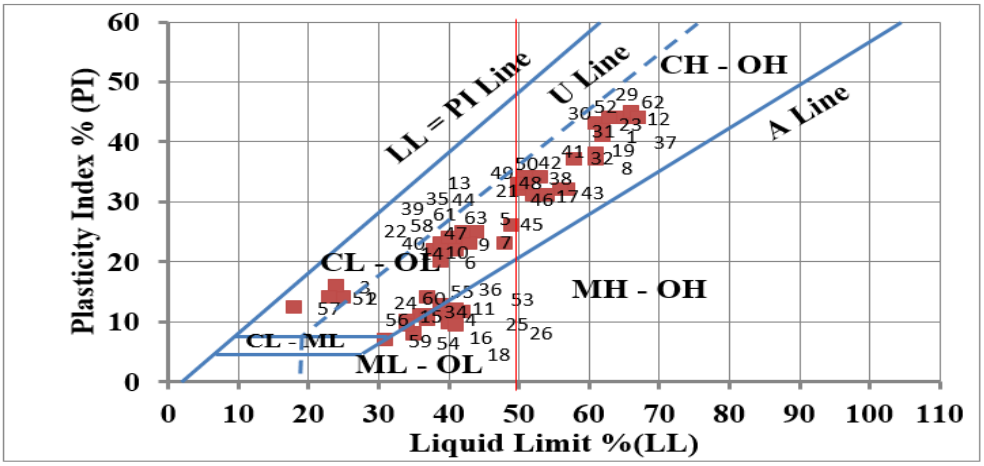

Fig. 10. Plasticity chart of soil in the study area of layer tow B2 depth (to 3 m).

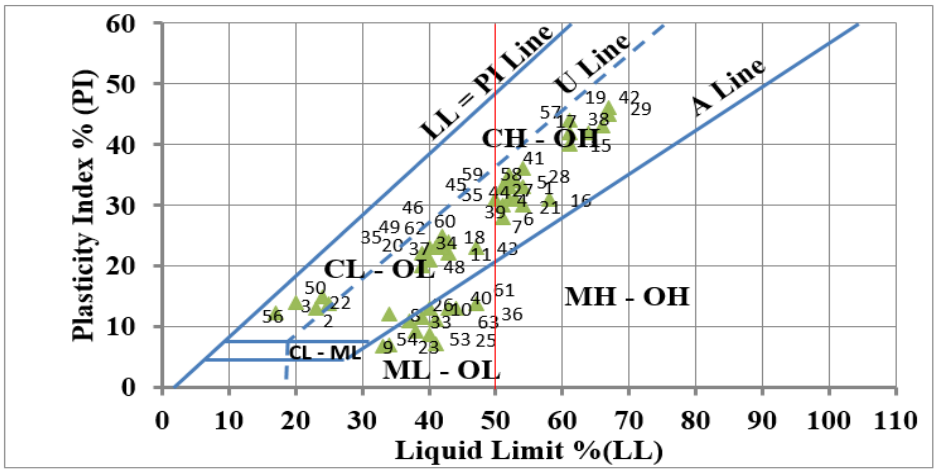

Fig. 11. Plasticity chart of soil in the study area of layer three B3 depth (to 5 m).

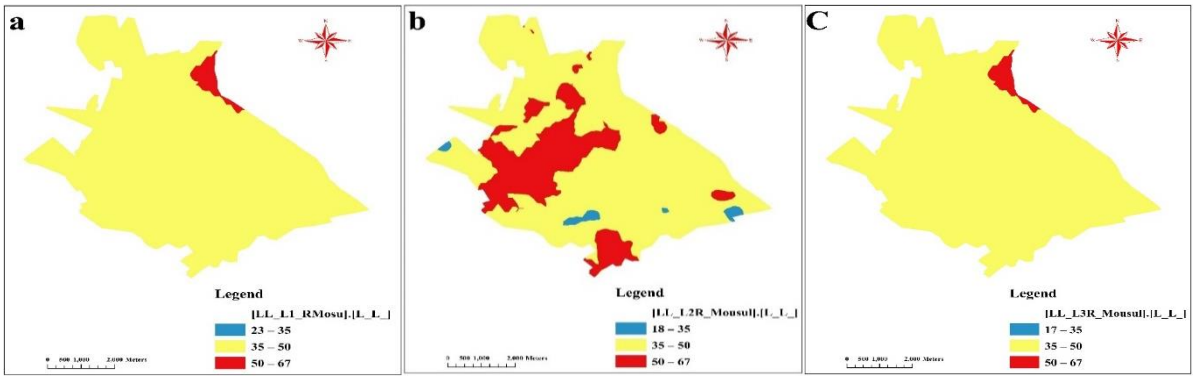

Fig. 12. Liquid limit for the study area by using interpolation in the ArcGIS program of three-layer depths; a- (1-1.5 m), b- (to 3 m), c- (to 5 m).

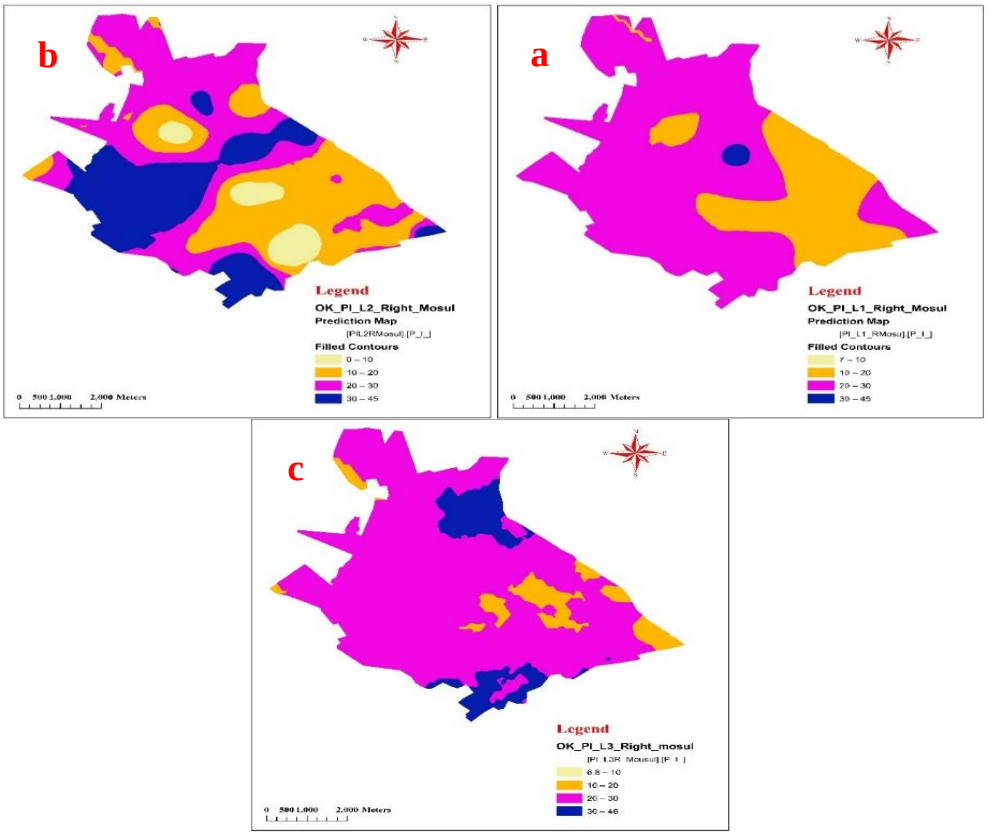

Fig. 13. Plasticity Index (PI) for municipal boundaries of Mosul right side according to interpolation in the ArcGIS program of three-layer depths; a- (1-1.5 m), b- (to 3 m), c- (to 5 m).

Activity of soil

The activity is used as an index property to determine the swelling potential of soil expansively (Skempton, 2024). Where the soil has an activity less than 0.75 is classified as inactive clays); and between (0.75 and 1.25) are (normal); while those activities greater than (1.25) are (active clays) (Holtz et al., 2011). In the study area, the ratio of activity is from 0.2 to 0.75, except for a few points having values more than 0.75, which indicates that the soil of the study area has poor clay activity.

Swelling potential

Any soil or rock material that has the potential for volume change because of an increase in its water content is called an expansive soil (Nelson and Miller, 1992).

Just a few minerals are accountable for engineering problems of swelling in rocks and soil. The clay minerals montmorillonite and vermiculite will cause problems when found in rock joints. Another problem mineral is anhydrite (anhydrous calcium sulfate, $CaSO_4$). In addition, salts found in evaporate deposits and some basalt types (fine-grained volcanic rock) can swell enough to create problems for overlying or neighboring structures (Goodman, 1989).

The fabric depends on the pressing method. If the soil is sheared repeatedly during compaction, as in the case of impact compaction, rather than just being compacted steadily, the fabric tends to be more directional than random, and this occurs more when the soil is at optimum wet than dry. (Holtz et al., 2011). Firoozi et al. (2016) referred to that proposed by Skempton (1953) a method to classify expansive potential for various types of soils by relating the plasticity index with the percent of clay fraction (passing 0.002 mm). Savage (2007) developed a method and applied a chart to evaluate a questionable soil to swell from soil plasticity, then developed by Al-Taie (2011).

By applying the chart of Savage (2007) and the developed equation to calculate Pg based on the result of study values on each of the three beds, the sample is distributed and classified based on the zoning of the swelling potential as shown in Figures 14, 15, and 16.

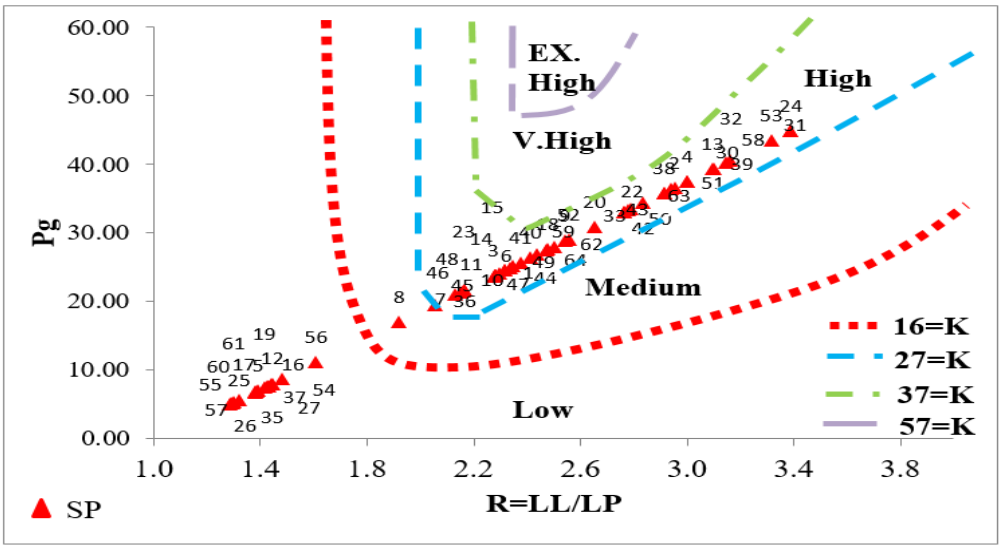

Fig. 14. Swelling potential from the relationship between R and Pg of soil in the municipal boundaries of Mosul, right side of layer one L1 (according to Savage, 2007).

Most of the plotted samples are in the zone of high swell potential, and some of them are in the low swelling potential zone, where fewer are in the medium swelling potential zone of the three depth layers, as shown in Figures 14, 15, and 16. The value of swelling potential is recorded in the Excel software and applying spatial interpolation by OK in the ArcGIS program and then classified as shown in figure (17 a, b, and c) for the study area showing that most areas have high swelling potential that ranges in value from (26) to (36). Furthermore, it is observed in small and scattered areas, particularly in the southeast, in all beds that the medium zone of swelling potential appears in the range between 16 and 26. The area of this zone decreases towards the deeper layers. Small and dispersed areas in layer one (L1) at a depth of 1.5 m in the central region and an extremely small area in the southeast of the study area have low swelling potential values (less than 16) (Fig. 17a, b, c).

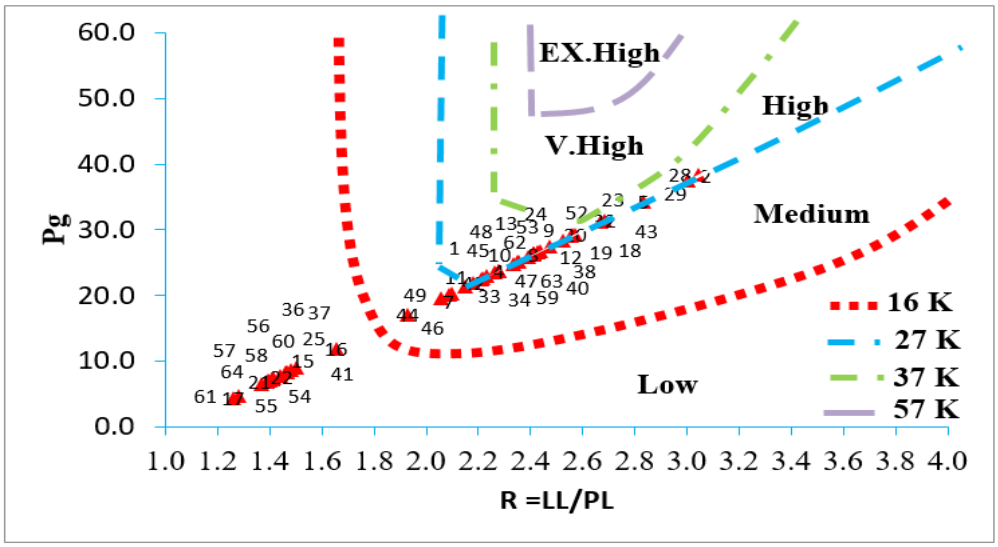

Fig. 15. Swelling potential from the relationship between R and Pg of soil in the municipal boundaries of Mosul, right side of layer two (L2), according to Savage (2007).

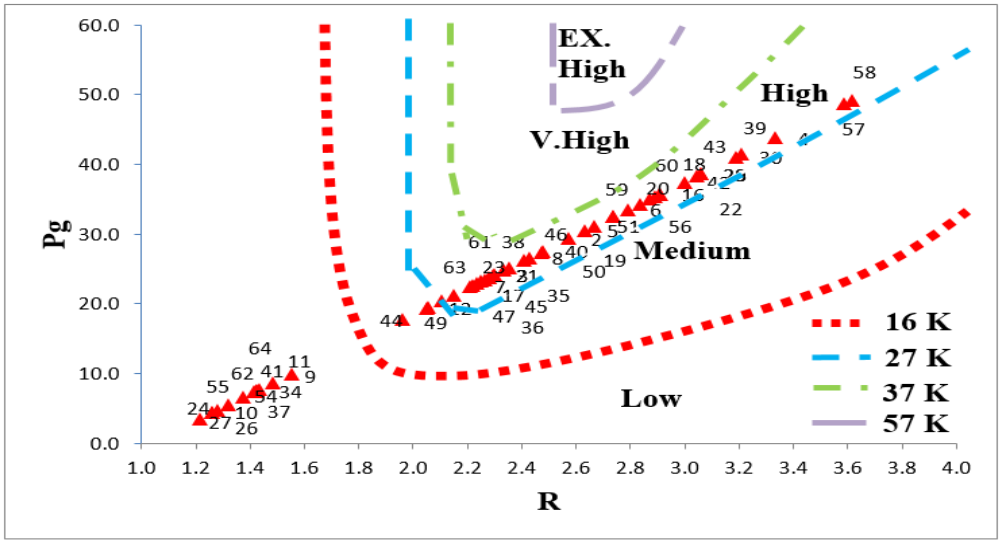

Fig. 16. Swelling potential from the relationship between R and Pg of soil in the municipal boundaries of Mosul, right side of layer three (L3), according to Savage (2007).

Water content

The water content (w) is the ratio of the weight of water to the weight of the solids in a given mass of soil. It is also known as natural water content or natural moisture content; this ratio is usually expressed as a percentage. When voids are filled with air, water content is equal to zero (dry soil) (Ranjana and Rao, 2000).

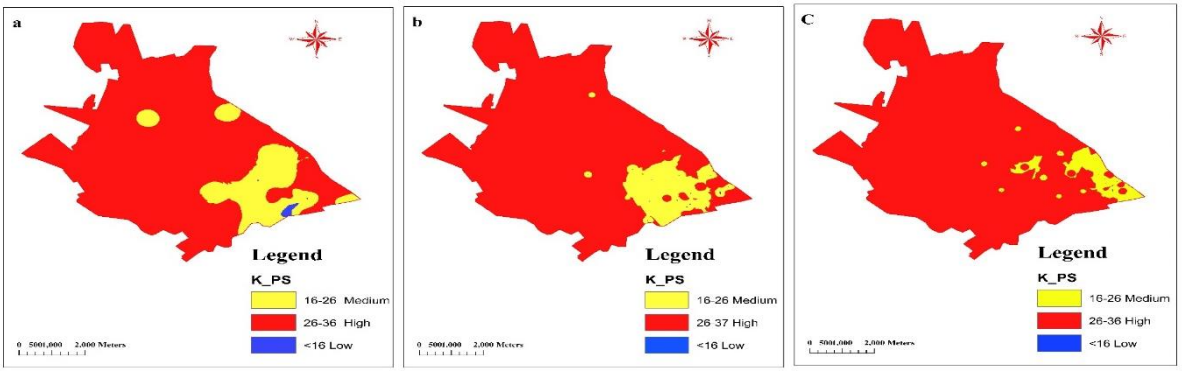

Fig. 17. Swelling potential of soil in municipal boundaries of Mosul, right side of the three-layer depths; a- (1-1.5 m), b- (to 3 m), c- (to 5 m).

Soil that holds more water indicates that it has more pores. Soil with more water has low strength because more water between soil particles reduces the shear strength of the soil (Ghosh, 2013).

The water content is applied by using OK interpolation (Fig. 18a, b, and c), as the figure shows that water content in the first layer is midlist from 5-10 in most of the eastern part and from 10-15. This distribution in the water content is reflected at the second and third beds, with a relative increase in the third bed indicating the soil at this bed is far from underground water in most of the study area. Water content decreased especially in the western part of the second and third beds, and then increased in the eastern part towards the river as it approached the groundwater level in some areas.

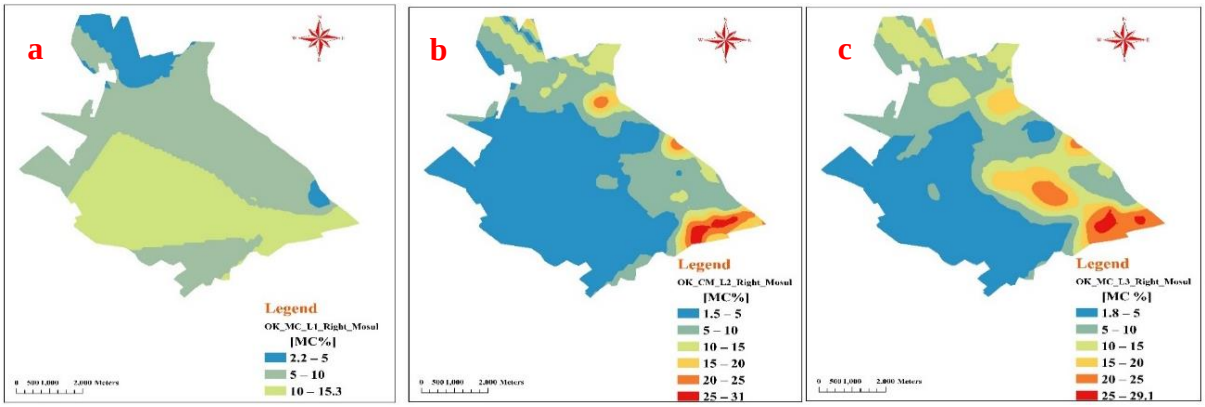

Fig. 18. Moisture content of Mosul right side according to interpolation in the ArcGIS program of three-layer depths; a- (1-1.5 m), b- (to 3 m), c- (to 5 m).

Dry and Wet Unit Weight

The solid particles are important in the soil, as they give the ability and support the soil structures (Venkatramaiah, 2006).

OK interpolates the value of wet and dry unit weight (Figs. 19, 20, and 21). A contrast between the first layer and from second and third layers is clear in (Figs. 20 and 21) showing that there is, as the dry and wet unit weight values in layer one decrease then increase towards the deeper layers, that which attributed to the proximity of the deeper layers from the groundwater level.

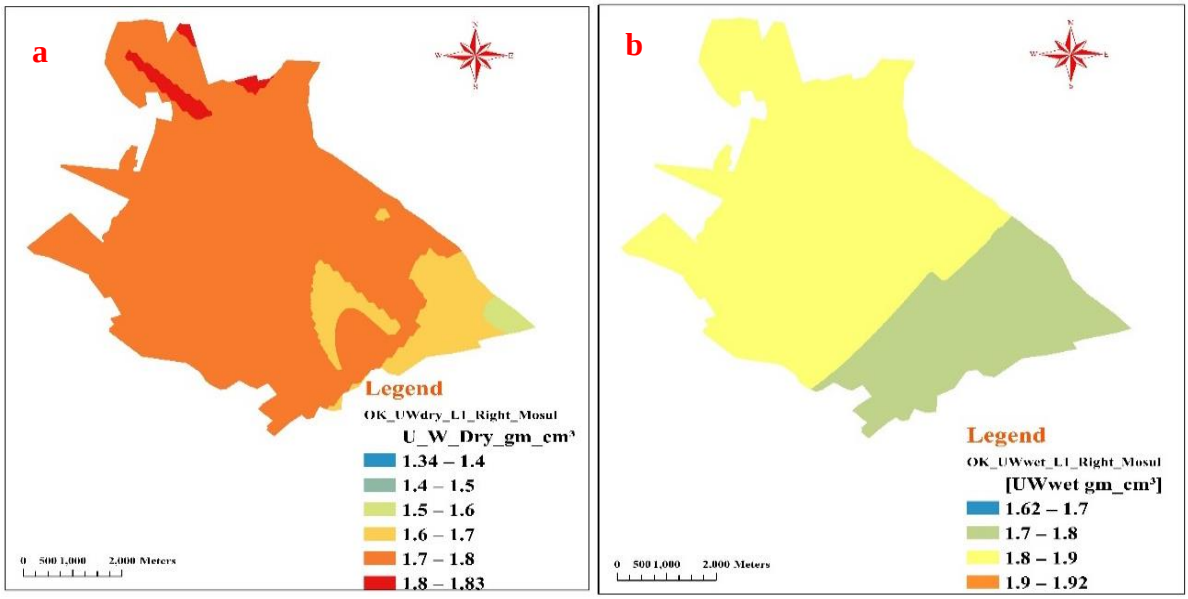

Fig. 19. a- Unit dry and b-unit wet distribution on the Mosul right side according to interpolation in ArcGIS program of layer one (L1) depths (1-1.5 m).

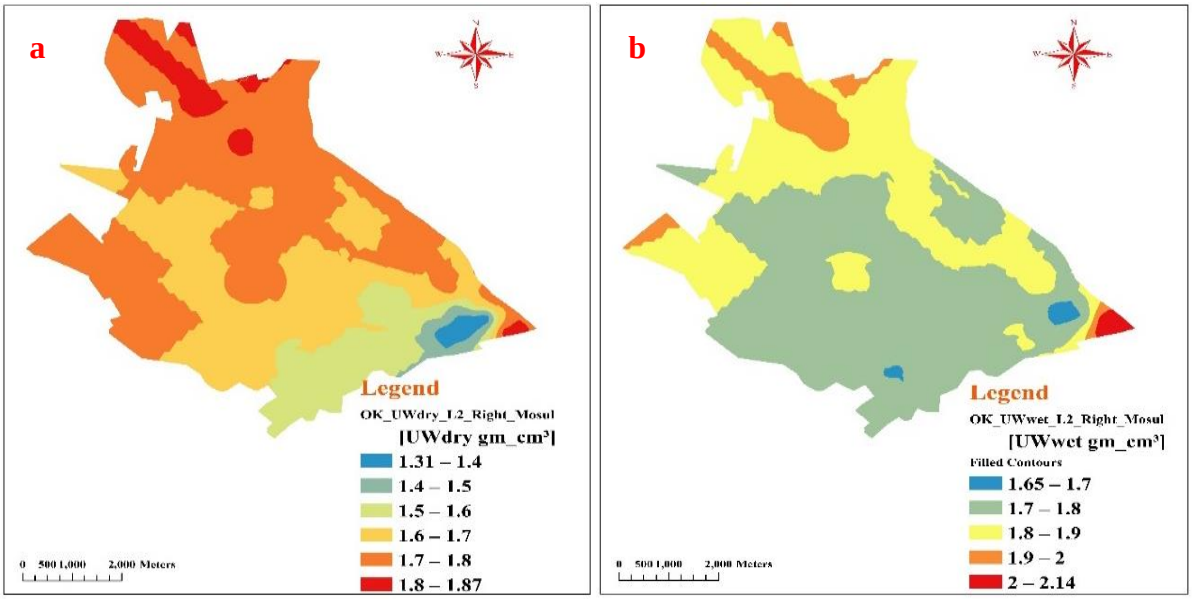

Fig. 20. a- unit dry and b-unit wet distribution on the Mosul right side according to interpolation in the ArcGIS program of layer two (L2) depths (to 3 m).

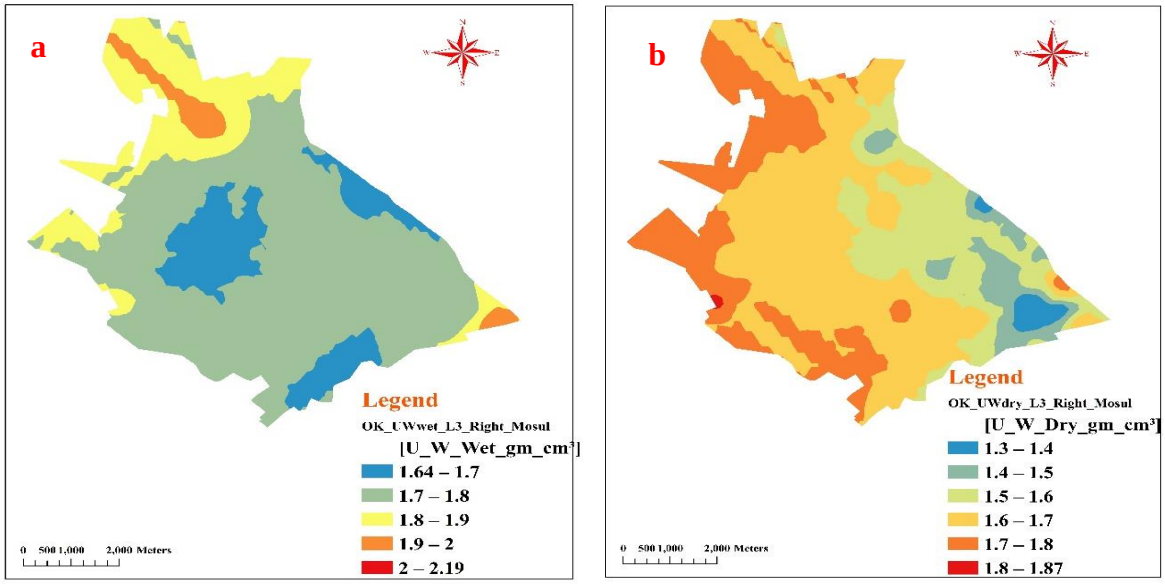

Fig 21. a- Unit dry and b- unit wet distribution on the Mosul right side according to interpolation in the ArcGIS program of layer three (L3) (to 5m depth).

Standard Penetration Test (SPT)(N) correction

The standard penetration test, the most widely used and affordable way to get subsurface data (both on land and offshore), was developed in 1927 (Bowell, 1996).

This study depends on the relationship between SPT and soil classification modified by Abubakar et al. (2015) according to Bowles (1996). Using OK interpolation for SPT values, the classification in spatial analysis tools in the ArcGIS program is used as illustrated in Figures 22a, b, and c, which displays the majority of the research area across all layers of moderately compact clay. Small areas in the second and third layers are described as compact to very compact clay, gravel, rock, or hard beds (Fig. 22 b and c). Additionally, a small area in the southwest of layer one is classified as soft clay (Fig. 22a). Some areas in the northern and fewer in the southern parts near the river are classified as compact to stiff clay, compact silt, silt, and loose sand, and moderately compact sand.

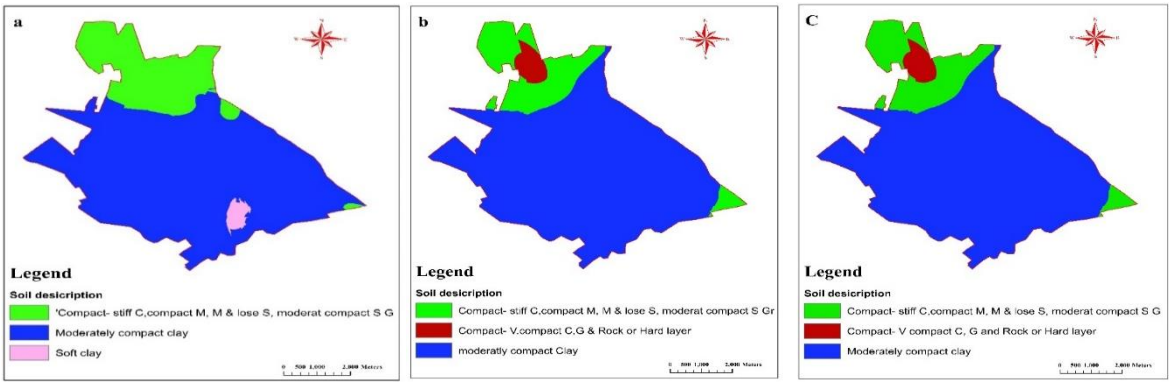

Fig. 22. Soil classification depending on SPT values as (Abubakar et al., 2015) according to Bowles (1996) for study area by interpolation in the ArcGIS program of three-layer depths; a- (1-1.5 m), b- (to 3 m), c- (to 5 m).

Bearing Capacity

The failure of bearing capacity is the representation of a foundation failure that occurs when the shear stresses in the soil exceed the shear strength of the soil (Kimmerling, 2002).

Many researchers calculated the equation of bearing capacity; the most commonly used equation is that developed by Terzaghi (1943) with modifications suggested by Meyerhof (1963). OK, ArcGIS interpolates the results of allowable bearing capacity.

The study area is classified depending on the relationship between bearing capacity and type of foundation according to IS-12070 (1987), as shown in Table 4, using in spatial analysis classification tool in the ArcGIS program as shown in Figure 23a, b, and c. According to Table 4 and depending on IS-12070 (1987), types of foundations are classified by a special analysis tool in ArcGIS as shown in Figures 23a, b, and c. Four types of foundations are distributed in the study area; in the northern part, the type suggestion is a combined or mat footing depth of 1.8 m, and along the northern east-west and some parts of southern east near the river are combined or mat footing. From the center to the south were deep piles of 3 m, and finally, in the southwest part were deep piles of 5 m.

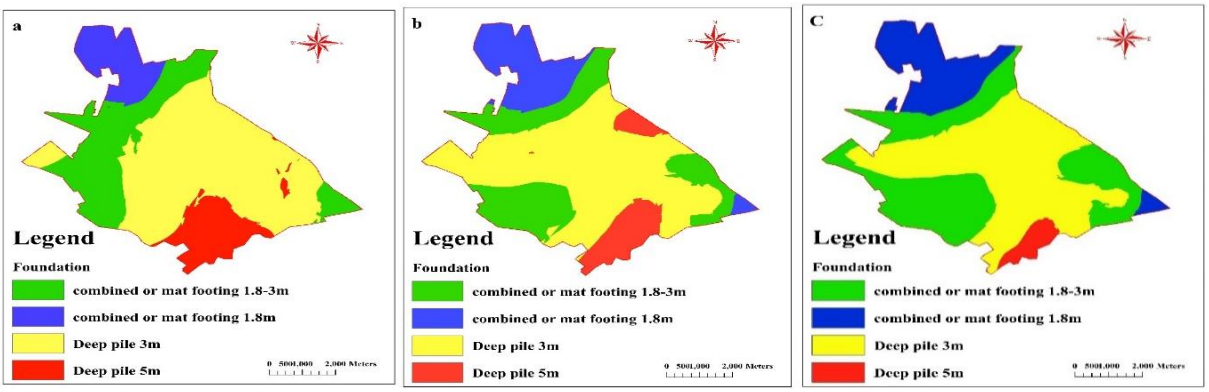

Fig. 23. Types of foundation depending on values of bearing capacity of soil for the study area by ArcGIS program of three-layer depths; a- (to 1.5 m), b- (to 3 m), c- (to 5 m) according to IS-12070 (1987).

Chemical Test

The chemical tests of soil samples are conducted to determine the levels of sulfates, chlorides, organic matter, calcium carbonate, pH, TSS, and gypsum.

The results show that the values of sulfate as SO_3 % range is (1.8 to 3.58) %, and gypsum and pH content are (5.61 to 11.28) % and (8.1 to 8.3) % respectively.

The Iraqi concrete laws classify the sulfates in soil and prescribe preventative measures for concrete. The SO_3 result indicates an intensive sulfate environment in all parts of each layer. This is additionally a result of the high gypsum content percentage.

The chloride content range is 0.03 to 0.04 %. This result indicates that all study areas should use pre-stressed concrete according to ACI 318-95.

Conversely, the range of organic matter found in soil samples is (1.6 to 3.89) %. With (3.98 to 7.31) % TSS (total suspended solids) and a high proportion of CaCO3 from (11 to 21) %.

For this case, the suggestion is to use sulfate-resistant Portland cement (SRPC) for the foundation and all concrete, in contact with soil covered on all sides of the concrete with a bitumen layer, with a thickness according to the choice of the designer, or a minimum cement content is 410 kg/m^3. The maximum free water/ cement ratio is 0.50 by weight when structures are above the water table. If a variable water table comes into contact, it is imperative to ascertain the appropriateness of using mix type 5 cement, asphalt, pitchy, or alternative impermeable foaming materials before making any required decisions.

Conclusions

The results for the three layers on the plasticity chart show that the data are distributed over three groups: (CH- high plasticity clay), (CL- Low plasticity clay), and (ML- low plasticity silt). Most areas of the three layers have a liquid limit between 30-50%, and the plasticity index increases towards deeper layers. The ratio of activity shows that the soil of the study area has poor clay activity in all layers in almost study area. High swelling potential dominated most of the study area, except the southern east parts, for each layer that had a medium swelling potential, and the area of this part decreased toward the deeper layers. The water content increases near the groundwater level. As well as the dry and wet unit weight values in layer one decrease, then increase towards the deeper layers, which was caused by the approach to the groundwater level and the deeper layers. The relationship between SPT and soil classification displays that the majority of the research area across all layers is moderately compact clay, while some areas in the northern and fewer in the southern parts near the river are classified as compact to stiff clay, compact silt, silt, and loose sand, and moderately compact sand. According to the bearing capacity, the foundation appears to increase in depth from the northeast, which has a foundation type of compact footing 1.8 m depth, to the southwest, which requires a deep pile 5 m depth. Finally, chemical tests show that all the study area layers have an intensive sulfate environment, and the chloride content is between 0.03 to 0.04%. This is due to the use of pre-stressed concrete type, also a high percentage of $CaCO_3$ and gypsum, and a high PH approaching 8.3.

Acknowledgments

The authors would like to express gratitude to the University of Mosul, Tikrit University, Iraq, and the Al-Mawarid Bureau for geological and geoengineering consultation for their support in completing this work.

References

Abdulrazaq, H.A. and Guedes, M.C., 2021. Post-War Sustainable Housing Design Strategies: The Case of Reconstruction in Iraq, Renewable Energy Environmental Sustainability, Vol. 6, pp. 1-22, https://doi.org/10.1051/rees/2021021.

Abubakar, M., Asrillah, I.K., Nugraha, G.S., 2015. Determining and Characterizing Bedrocks Using Geo-Electrical and Geotechnical Methods at Belawan - North Sumatra, Electronic Journal of Geotechnical Engineering, Vol. 20, Issue 3, pp. 1076-1085, https://www.researchgate.net/publication/283019548.

Adeeb, H.Gh.M., 1988. Structure and Stratigraphy of Mosul City – The Right Bank, Unpublished. MSc Thesis. College of Science, University of Mosul, Iraq, 168 P. (In Arabic).

Aldefae, A.H., Mohammed, J., and Saleem, H.D., 2020. Digital Maps of Mechanical Geotechnical Parameters Using GIS, Civil and Environmental Engineering Research Article, Vol. 7, P 1779563, https://doi.org/10.1080/23311916.2020. 1779563.

Al-Jaber, F.Kh., 1997. Geomorphology and Geoengineering of Mosul City by Using Remote Sensing Techniques, Unpublished MSc Thesis, College of Science, University of Mosul, Iraq, 168 P. (In Arabic).

Al-Jawadi, A.S., Saleh, D.G. and Younis, A.A., 2022. Protection and Management of the Destroyed Heritage in the Old City of Mosul, Northern Iraq, Iraqi Geological Journal, Vol. 55, No. 2F, pp. 224-233, https://doi.org/10.46717/igj.55.2F.16ms-2022-12-31.

Al-Mosawy, S.K., Al-Jaberi, A.A., Alrobaee, T.R. and Al-Khafaji, A.S., 2021. Urban Planning and Reconstruction of Cities Post-Wars by the Approach of Events and Response Images, Civil Engineering Journal, Vol. 7, No. 11, P. 1836- 1852, http://dx.doi.org/10.28991/cej-2021-03091763.

Alrobaee, T.R. and Al Yousif, I.J., 2018. The Schematic Thought of Cities beyond the Hermann Theory, Iraqi Journal of Architecture and Planning, Vol. 14, Issue 2, pp. 232-246. (In Arabic).

Al-Taie, A.J., 2016. Practical Aid to Identify and Evaluate Plasticity, Swelling and Collapsibility of the Soil Encountered in Badrah, Shatra and Nassirya Cities, Journal of Engineering and Development, Vol. 20, No. 1, pp. 38-47.

Boloorani, A.D., Darvishi, M., Weng, Q. and Liu, X., 2021. Post-War Urban Damage Mapping Using InSAR: The Case of Mosul City in Iraq, ISPRS Int. J. Geo-Inf., Vol. 10, P. 140. https://doi.org/10.3390/ijgi10030140, https://www.mdpi.com/journal/ijgi

Boumpoulis, V., Michalopoulou, M. and Depountis, N., 2023. Comparison Between Different Spatial Interpolation Methods for the Development of Sediment Distribution Maps in Coastal Areas, Earth Science Informatics, Vol. 16, pp. 2069-2087, https://doi.org/10.1007/s12145-023-01017-4.

Bowles, J.E. and Guo, Y., 1996. Foundation Analysis and Design, Vol. 5, 127 P., New York: McGraw-Hill Companies, Inc., 5th Edition.

Firoozi, A.A., Asghar, A.F. and Baghini, M.S., 2016. A Review of Clayey Soils, Asian Journal of Applied Sciences, Vol. 04, Issue 06, pp. 1319- 1330.

Ghosh, R., 2013. Effect of Soil Moisture in the Analysis of Undrained Shear Strength of Compacted Clayey Soil, Journal of Civil Engineering and Construction Technology, Vol. 4, No. 1, pp. 23-31.

Goodman, R.E., 1989. Introduction to Rock Mechanics, John Wiley and Sons, 2nd Edition, 562 P.

Holtz, R.D., Kovacs, W.D., Sheahan, T.C., 2011. An Introduction to Geotechnical Engineering, Pearson Education, Inc., 2nd Edition, 853 P. https://doi.org/10.5194/egusphere-2024-1607.

Ikara, A.I., Umar, Y.H. and Dauda, B.D., 2022. Mapping of Geotechnical Properties Using ArcGIS: A Case Study of Abubakar Tafawa Balewa University, Bauchi, Gubi Campus, Iconic Research and Engineering Journals, Vol. 5, Issue 9.

IS, 12070, 1987. Code of Practice for Design and Construction of Shallow Foundations on Rocks, Published by Bureau of Indian Standards, New Delhi, India.

Justyna, K., Kuśnierz-Krupa, D., Ivashko, Y. and Savelieva, L., 2020. Methods of Revitalizing Historical Industrial Facilities-International Experience. Wiadomosci Konserwatorskie. Vol. 2020. Wiadomości Konserwatorskie, https://doi.org/10.48234/WK62INDUSTRIAL.

Kawther, K.K. and Hassan, R.H., 2022. Sustainable Urban Space Strategies in the Reconstruction of Destroyed Cities After the Wars, Journal of Engineering Science and Technology, Taylor's University, Vol. 17, No. 6, pp. 4163-4186.

Kimmerling R.E., 2002. Geotechnical Engineering Circular No.6 Shallow Foundations, Technical Report Documentation, Office of Bridge Technology of Federal Highway Administration, 310 P.

Nelson J.D. and Miller D.J., Book Review: Expensive Soil-Problems and Practice in Foundation and Pavement Engineering, 1992. International Journal for Numerical and Analytical Methods in Geomechanics, New York, Vol. 17, pp. 745-746.

Ranjan G. and Rao A.S.R., 2000. Basic and Applied Soil Mechanics, New Age International Publisher, 2nd Edition, 153 P.

Savage P.F., 2007. Evaluation of Possible Swelling Potential of Soil, the 26th Southern African Transport Conference, pp. 277-283.

Sissakian, V.K., Hagopian, D.H. and Hasan, E.A., 1995. Geological Map of A--Mosul Quadrangle, Sheet NJ-38-13, State Establishment of Geological Survey and Mining, Baghdad, Iraq.

Truedinger A., Birkmann J., Fleischhauer M. and Ferreira C., 2024. Sensitive infrastructures and people with disabilities – Key Issues when Strengthening Resilience in Reconstruction, Egusphere.

UN-Habitat for Humanity, 2019, Initial Planning Framework for the Reconstruction of Mosul; HH: Atlanta, GA, USA.

Venkatramaiah C., 2006. Geotechnical Engineering, New Age International (P), Third Edition.